

Next-to-leading-order correction to pion form factor in k_T factorization

Hsiang-nan Li^{a,b,c}, Yue-Long Shen^{a,d}, Yu-Ming Wang^{e,f}, Hao Zou^f

^a*Institute of Physics, Academia Sinica, Taipei, Taiwan 115, Republic of China*

^b*Department of Physics, National Cheng-Kung University, Tainan, Taiwan 701, Republic of China*

^c*Department of Physics, National Tsing-Hua University, Hsinchu, Taiwan 300, Republic of China*

^d*College of Information Science and Engineering,*

Ocean University of China, Qingdao, Shandong 266100, P.R. China

^e*Theoretische Physik 1, Fachbereich Physik, Universität Siegen, D-57068 Siegen, Germany*

^f*Institute of High Energy Physics and Theoretical Physics Center
for Science Facilities, P.O. Box 918(4) Beijing 100049, China*

We calculate next-to-leading-order (NLO) correction to the pion electromagnetic form factor at leading twist in the k_T factorization theorem. Partons off-shell by k_T^2 are considered in both quark diagrams and effective diagrams for the transverse-momentum-dependent (TMD) pion wave function. The light-cone singularities in the TMD pion wave function are regularized by rotating the Wilson lines away from the light cone. The soft divergences from gluon exchanges among initial- and final-state partons cancel exactly. We derive the infrared-finite k_T -dependent NLO hard kernel for the pion electromagnetic form factor by taking the difference of the above two sets of diagrams. Varying the renormalization and factorization scales, we find that the NLO correction is smaller, when both the scales are set to the invariant masses of internal particles: it becomes lower than 40% of the leading-order (LO) contribution for momentum transfer squared $Q^2 > 7 \text{ GeV}^2$. It is observed that the NLO leading-twist correction does not play an essential role in explaining the experimental data, but the LO higher-twist contribution does.

PACS numbers: 12.38.Bx, 12.38.Cy, 12.39.St

I. INTRODUCTION

The k_T factorization theorem [1–6] in perturbative QCD (PQCD) has caught a lot of attention recently (see [7, 8] for its recent applications). How to derive a hard kernel beyond leading order (LO) in the k_T factorization theorem is one of the important subjects. We have proposed the prescription that partons in both QCD quark diagrams and effective diagrams for transverse-momentum-dependent (TMD) hadron wave functions are off mass shell by k_T^2 [9]. Since the gauge dependence cancels between the two sets of diagrams, their difference defines a gauge-invariant hard kernel. The gauge invariance of the k_T factorization theorem has been investigated in [10, 11], and proved in [12]. The light-cone singularities, appearing in the naive definition of TMD wave functions, are regularized by rotating the Wilson lines away from the light cone [13–15]. Following the above prescription, the next-to-leading-order (NLO) correction to the pion transition form factor associated with the process $\pi\gamma^* \rightarrow \gamma$ has been calculated at leading twist [11]. Both the large double logarithms $\alpha_s \ln^2 k_T$ and $\alpha_s \ln^2 x$, x being a parton momentum fraction, were identified. The former is absorbed into the pion wave function and summed to all orders in α_s by the k_T resummation, and the latter is absorbed into a jet function and summed to all orders in α_s by the threshold resummation.

In this paper we shall extend the framework to the more complicated pion electromagnetic form factor associated with the process $\pi\gamma^* \rightarrow \pi$. Our work represents the first NLO study of this quantity at leading twist in the k_T factorization theorem. The NLO correction to the pion form factor has been evaluated in the collinear factorization theorem by several groups [16–24]. For $\pi\gamma^* \rightarrow \pi$, not only the collinear divergences from gluon emissions collimated to the initial- and final-state pions, but also the soft divergences from gluon exchanges between the two pions exist. Therefore, it is nontrivial to demonstrate that the collinear divergences in the quark diagrams are cancelled by those in the pion wave functions, and the soft divergences cancel among themselves. The computation of the box and pentagon diagrams for the pion form factor is also technically involved. The renormalization scale μ and the factorization scale μ_f are introduced by higher-order corrections to the quark diagrams and to the effective diagrams, respectively. We shall show that the NLO correction to the pion form factor is smaller, when both the scales are set to the invariant masses of internal particles as postulated in [5, 25]: it becomes lower than 40% of the LO contribution for momentum transfer squared $Q^2 > 7 \text{ GeV}^2$. The variation of the pion form factor with μ and μ_f gives an estimate of the theoretical uncertainty in our analysis.

Another related subject concerns the shape of the pion distribution amplitudes. It has been pointed out [26] that the recent BaBar data of the pion transition form factor $F_{\pi\gamma}(Q^2)$ [27] at low (high) Q^2 indicate an asymptotic (flat) leading-twist, i.e., twist-2 pion distribution amplitude. However, a pion distribution amplitude ought to be universal.

These seemingly contradictory observations have been reconciled in the k_T factorization theorem [26]: the increase of the measured $Q^2 F_{\pi\gamma}(Q^2)$ for $Q^2 > 10 \text{ GeV}^2$ was explained by convoluting a k_T -dependent hard kernel with a flat pion distribution amplitude. The low Q^2 data were accommodated by including the threshold resummation of $\alpha_s \ln^2 x$, which provides a strong suppression at the endpoints of x . The suppression becomes stronger as Q^2 decreases. That is, the twist-2 pion distribution amplitude multiplied by the threshold resummation factor behaves like the asymptotic model at low Q^2 effectively. In this work we shall show that the asymptotic models for both the twist-2 and two-parton twist-3 pion distribution amplitudes also lead to results in better agreement with the data of the pion form factor at low Q^2 , compared to those from the non-asymptotic models. It is found that the NLO twist-2 correction does not play an essential role in accounting for the data, but the contribution from the LO two-parton twist-3 pion distribution amplitudes does, a conclusion the same as drawn in [28].

In Sec. II we calculate the $O(\alpha_s^2)$ QCD quark diagrams, the $O(\alpha_s)$ effective diagrams for the TMD pion wave function, and their convolution with the $O(\alpha_s)$ hard kernel, considering partons off-shell by k_T^2 . Since the k_T factorization theorem is appropriate for QCD processes dominated by contributions from small x [9], we shall keep only terms in leading power of x . Taking the difference between the two sets of diagrams, we derive the NLO k_T -dependent hard kernel for the pion form factor. Section III contains the numerical investigation, in which we obtain the partial contributions to the pion form factor from different twists and orders, and the relative importance of the LO and NLO twist-2 contributions. We also examine the dependence of our results on the renormalization and factorization scales, and on the shape of the pion distribution amplitudes. Section IV is the conclusion.

II. NLO CORRECTIONS

In this section we compute the $O(\alpha_s^2)$ quark diagrams in QCD and the $O(\alpha_s)$ effective diagrams for the pion wave function in the Feynman gauge, and then derive the NLO hard kernel for the pion electromagnetic form factor in the k_T factorization theorem. The momentum P_1 (P_2) of the initial-state (final-state) pion is chosen as $P_1 = (P_1^+, 0, \mathbf{0}_T)$ ($P_2 = (0, P_2^-, \mathbf{0}_T)$). The anti-quark \bar{q} carries the momentum $k_1 = (x_1 P_1^+, 0, \mathbf{k}_{1T})$ in the initial state and $k_2 = (0, x_2 P_2^-, \mathbf{k}_{2T})$ in the final state, as indicated by the LO quark diagrams in Fig. 1. The parton virtuality k_T^2 regularizes the collinear and soft divergences into the logarithm $\ln k_T^2$. We shall focus only on Fig. 1(a), since the NLO correction to Fig. 1(b) can be obtained from that to Fig. 1(a) by exchanging the kinematic variables of the two pions. The NLO corrections to the other two LO quark diagrams with the virtual photon attaching to the anti-quark line are then obtained via the variable exchanges between the quark and the anti-quark. According to the hierarchy $Q^2 \gg xQ^2 \gg k_T^2$ in the small- x region, we keep only those terms that do not vanish in the $x \rightarrow 0$ and $k_T \rightarrow 0$ limit.

Figure 1(a) leads to the amplitude

$$\begin{aligned} H^{(0)}(x_1, k_{1T}, x_2, k_{2T}, Q^2) &= -g^2 C_F \frac{N_c}{(\sqrt{2N_c})^2} \frac{\text{Tr}[\gamma_\nu \gamma_5 P_2 \gamma^\nu (P_2 - k_1) \gamma_\mu P_1 \gamma_5]}{(P_2 - k_1)^2 (k_1 - k_2)^2}, \\ &= g^2 C_F \frac{\text{Tr}(P_2 P_1 \gamma_\mu P_1)}{Q^2 (x_1 x_2 Q^2 + |\mathbf{k}_{1T} - \mathbf{k}_{2T}|^2)}, \end{aligned} \quad (1)$$

where N_c is the number of colors, C_F is a color factor, $P_1 \gamma_5 / \sqrt{2N_c}$ and $\gamma_5 P_2 / \sqrt{2N_c}$ are the twist-2 spin structures of the initial- and final-state pions, respectively, and $Q^2 \equiv 2P_1 \cdot P_2$ is the momentum transfer squared from the virtual photon. To reach the last line in Eq. (1), we have applied the hierarchy $x_1 Q^2 \gg k_{1T}^2$ to the internal quark propagator. The denominator $x_1 x_2 Q^2 + |\mathbf{k}_{1T} - \mathbf{k}_{2T}|^2$ comes from the virtuality of the LO hard gluon. The $|\mathbf{k}_{1T} - \mathbf{k}_{2T}|^2$ term may not be negligible compared to $x_1 x_2 Q^2$ in the small- x region, so it is retained.

The NLO hard kernel $H^{(1)}$ is defined, in the k_T factorization theorem, by [9]

$$\begin{aligned} H^{(1)}(x_1, k_{1T}, x_2, k_{2T}, Q^2) &= G^{(1)}(x_1, k_{1T}, x_2, k_{2T}, Q^2) \\ &\quad - \int dx'_1 d^2 k'_{1T} \Phi^{(1)}(x_1, k_{1T}; x'_1, k'_{1T}) H^{(0)}(x'_1, k'_{1T}, x_2, k_{2T}, Q^2) \\ &\quad - \int dx'_2 d^2 k'_{2T} H^{(0)}(x_1, k_{1T}, x'_2, k'_{2T}, Q^2) \Phi^{(1)}(x_2, k_{2T}; x'_2, k'_{2T}), \end{aligned} \quad (2)$$

where $G^{(1)}$ denotes the NLO quark diagrams associated with Fig. 1(a), and $\Phi^{(1)}$ collects the $O(\alpha_s)$ effective diagrams for the twist-2 quark-level wave function [9, 29]

$$\Phi(x_1, k_{1T}; x'_1, k'_{1T}) = \int \frac{dy^-}{2\pi} \frac{d^2 y_T}{(2\pi)^2} e^{-ix'_1 P_1^+ y^- + i\mathbf{k}'_{1T} \cdot \mathbf{y}_T} \langle 0 | \bar{q}(y) W_y(n)^\dagger I_{n,y,0} W_0(n) \not{n} \gamma_5 q(0) | q(P_1 - k_1) \bar{q}(k_1) \rangle. \quad (3)$$

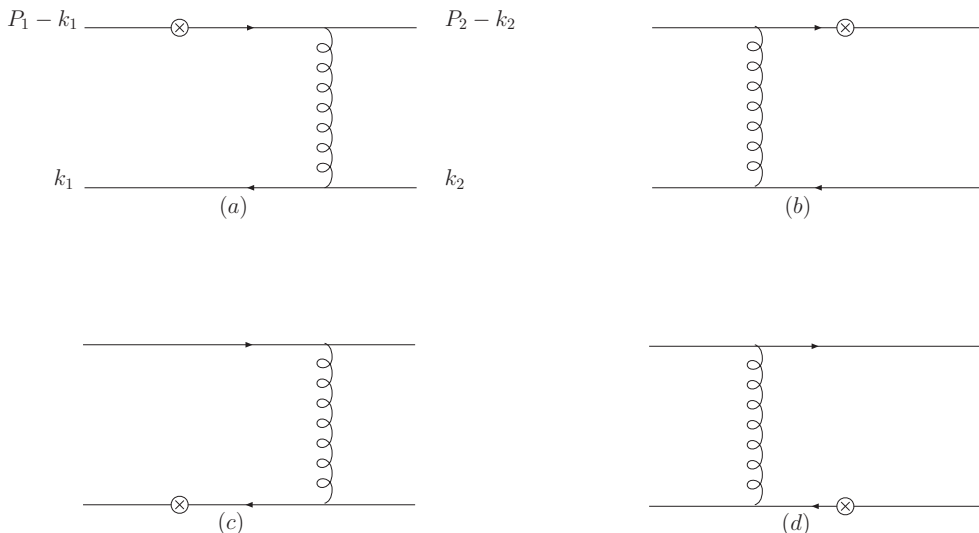


FIG. 1: Leading-order quark diagrams for $\pi\gamma^* \rightarrow \pi$ with \otimes representing the virtual photon vertex.

In the above expression $y = (0, y^-, \mathbf{y}_T)$ is the coordinate of the anti-quark field \bar{q} , $n_- = (0, 1, \mathbf{0}_T)$ is a null vector along P_2 , $|q(P_1 - k_1)\bar{q}(k_1)\rangle$ is the leading Fock state of the pion, and the Wilson line $W_y(n)$ with $n^2 \neq 0$ is written as

$$W_y(n) = P \exp \left[-ig \int_0^\infty d\lambda n \cdot A(y + \lambda n) \right]. \quad (4)$$

The two Wilson lines $W_y(n)$ and $W_0(n)$ are connected by a vertical link $I_{n;y,0}$ at infinity [30, 31]. Equation (3) will generate additional light-cone singularities from the region with a loop momentum collinear to n_- , as the Wilson line direction approaches the light cone, i.e., as $n \rightarrow n_-$ [13]. That is, n^2 serves as an infrared regulator for the light-cone singularities.

A. NLO Quark Diagrams

We first calculate the NLO corrections to Fig. 1(a) in the k_T factorization theorem, which come from Figs. 2, 3, and 4 for the self-energy corrections, the vertex corrections, and the box and pentagon diagrams, respectively. The ultraviolet poles are identified in the dimensional reduction [32] in order to avoid the ambiguity from handling the matrix γ_5 . To simplify the expressions, we define the following dimensionless ratios

$$\begin{aligned} \delta_1 &= \frac{k_{1T}^2}{Q^2}, & \delta_2 &= \frac{k_{2T}^2}{Q^2}, \\ \delta_{12} &= \frac{x_1 x_2 Q^2 + |\mathbf{k}_{1T} - \mathbf{k}_{2T}|^2}{Q^2}. \end{aligned} \quad (5)$$

Terms suppressed by powers of x or δ will be dropped in the NLO corrections.

The self-energy corrections to the four external quarks in Figs. 2(a)-2(d) give

$$G_{2a,2b}^{(1)} = -\frac{\alpha_s C_F}{8\pi} \left(\frac{1}{\epsilon} + \ln \frac{4\pi\mu^2}{\delta_1 Q^2 e^{\gamma_E}} + 2 \right) H^{(0)}, \quad (6)$$

$$G_{2c,2d}^{(1)} = -\frac{\alpha_s C_F}{8\pi} \left(\frac{1}{\epsilon} + \ln \frac{4\pi\mu^2}{\delta_2 Q^2 e^{\gamma_E}} + 2 \right) H^{(0)}, \quad (7)$$

where $1/\epsilon$ represents the ultraviolet pole, μ is the renormalization scale, and γ_E is the Euler constant. The collinear divergences in Figs. 2(a)-2(d) are regularized into the infrared logarithms $\ln \delta$. The self-energy correction to the internal quark in Fig. 2(e) leads to

$$G_{2e}^{(1)} = -\frac{\alpha_s C_F}{4\pi} \left(\frac{1}{\epsilon} + \ln \frac{4\pi\mu^2}{x_1 Q^2 e^{\gamma_E}} + 2 \right) H^{(0)}. \quad (8)$$

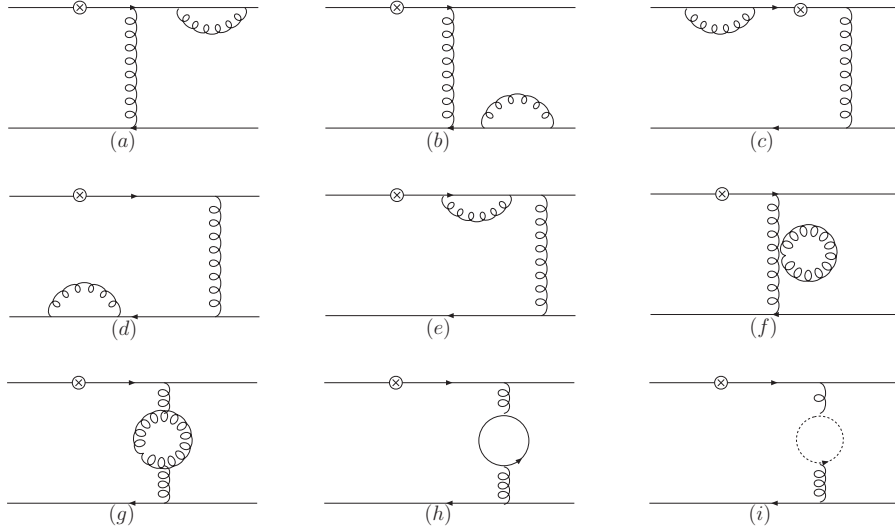


FIG. 2: Self-energy diagrams.

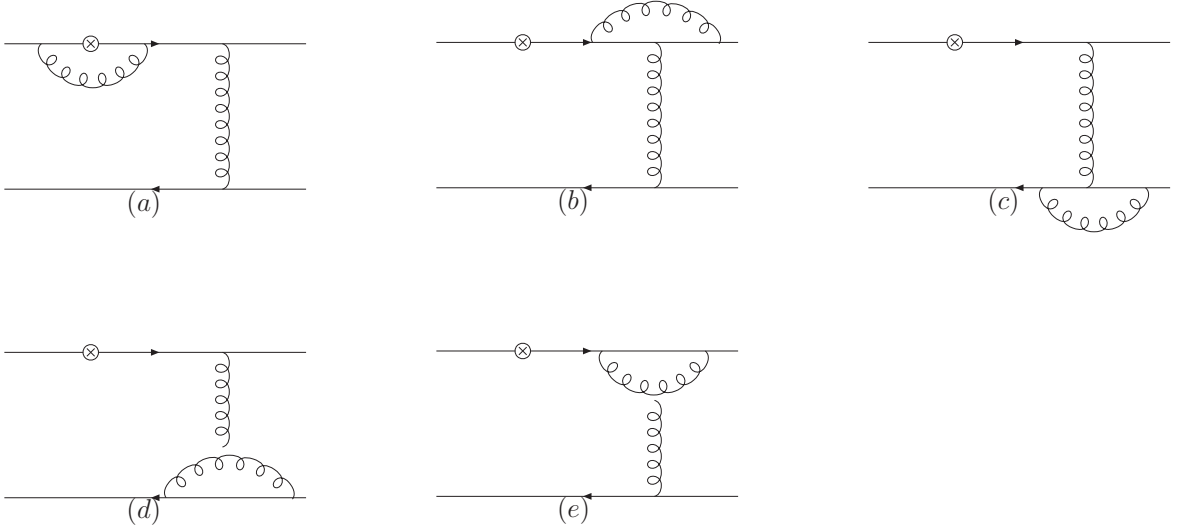


FIG. 3: Vertex-correction diagrams.

The ultraviolet poles in Eqs. (6) and (7) are half of that in Eq. (8), because an additional factor 1/2 is associated with an external particle. The internal quark is off-shell by the invariant mass squared $x_1 Q^2$, which replaces the arguments k_T^2 of the infrared logarithms in Eqs. (6) and (7). The self-energy correction to the hard gluon, summing the quark-, gluon- and ghost-loop contributions in Figs. 2(f)-2(i), is written as

$$G_{2f+2g+2h+2i}^{(1)} = \frac{\alpha_s}{4\pi} \left(\frac{5}{3} N_c - \frac{2}{3} N_f \right) \left(\frac{1}{\epsilon} + \ln \frac{4\pi\mu^2}{\delta_{12} Q^2 e^{\gamma_E}} \right) H^{(0)}, \quad (9)$$

with N_f being the number of quark flavors. In this case the logarithm depends on the invariant mass squared $\delta_{12} Q^2$ of the hard gluon.

The results from the five diagrams Figs. 3(a)-3(e) for the vertex corrections are summarized as

$$G_{3a}^{(1)} = \frac{\alpha_s C_F}{4\pi} \left(\frac{1}{\epsilon} + \ln \frac{4\pi\mu^2}{Q^2 e^{\gamma_E}} + 2 \right) H^{(0)}, \quad (10)$$

$$G_{3b}^{(1)} = -\frac{\alpha_s}{8\pi N_c} \left(\frac{1}{\epsilon} + \ln \frac{4\pi\mu^2}{x_1 Q^2 e^{\gamma_E}} + 2 \ln \frac{x_1}{\delta_2} + \frac{7}{2} \right) H^{(0)}, \quad (11)$$

$$G_{3c}^{(1)} = -\frac{\alpha_s}{8\pi N_c} \left(\frac{1}{\epsilon} + \ln \frac{4\pi\mu^2}{\delta_{12}Q^2 e^{\gamma_E}} - 2 \ln \frac{\delta_{12}}{\delta_1} \ln \frac{\delta_{12}}{\delta_2} + 2 \ln \frac{\delta_{12}^2}{\delta_1\delta_2} - \frac{2\pi^2}{3} + \frac{11}{2} \right) H^{(0)}, \quad (12)$$

$$G_{3d}^{(1)} = \frac{\alpha_s N_c}{8\pi} \left(\frac{3}{\epsilon} + 3 \ln \frac{4\pi\mu^2}{\delta_{12}Q^2 e^{\gamma_E}} + 2 \ln \frac{\delta_{12}^2}{\delta_1\delta_2} + \frac{23}{2} \right) H^{(0)}, \quad (13)$$

$$G_{3e}^{(1)} = \frac{\alpha_s N_c}{8\pi} \left[\frac{3}{\epsilon} + 3 \ln \frac{4\pi\mu^2}{x_1 Q^2 e^{\gamma_E}} + 2 \ln \frac{x_1}{\delta_2} \left(1 - \ln \frac{x_1}{\delta_{12}} \right) + \ln \frac{x_1}{\delta_{12}} - \frac{2}{3}\pi^2 + \frac{7}{2} \right] H^{(0)}. \quad (14)$$

The ultraviolet poles in the self-energy and vertex corrections are summed into

$$\frac{\alpha_s}{4\pi} \left(11 - \frac{2}{3}N_f \right) \frac{1}{\epsilon}, \quad (15)$$

for $N_c = 3$, which is the same as obtained in [22]. This pole term determines the renormalization-group (RG) evolution of the coupling constant α_s .

The loop correction $G_{3a}^{(1)}$ to the photon vertex does not contain an infrared logarithm, because of the sequence of the γ -matrices in the fermion flow. The correction $G_{3b}^{(1)}$ to the upper gluon vertex contains only the infrared logarithm associated with the final-state pion. The other end of the radiative gluon attaches to the internal quark line, so $G_{3b}^{(1)}$ depends on $x_1 Q^2$, and does not generate a double logarithm. The correction to the lower gluon vertex in Fig. 3(c) depends on the momentum transfer squared $\delta_{12} Q^2$ from the LO hard gluon, and on the two infrared regulators δ_1 and δ_2 from the incoming and outgoing partons. The expression of $G_{3c}^{(1)}$ is symmetric under the exchange of δ_1 and δ_2 as expected. The $\ln(\delta_{12}/\delta_1) \ln(\delta_{12}/\delta_2)$ term is not a large double logarithm in the small- x region, where $\ln \delta_1 \ln \delta_2$ arises from the soft region of the radiative gluon. It is obvious from the convolutions of $\Phi^{(1)}$ and $H^{(0)}$ in Eq. (2) that this soft logarithm can not be cancelled by the infrared logarithms in the effective diagrams: there is no chance for $\ln \delta_1$ associated with the initial-state pion and $\ln \delta_2$ associated with the final-state pion to appear in a product. Therefore, cancellation must occur within this type of soft logarithms as demonstrated below.

The triple-gluon vertex correction $G_{3d}^{(1)}$ also depends on the scale $\delta_{12} Q^2$, and contains the same infrared logarithm $\ln(\delta_{12}^2/\delta_1\delta_2)$ as in $G_{3c}^{(1)}$ but with different color factors. Their sum is proportional to C_F : $-1/N_c + N_c = 2C_F$, implying the factorization of this infrared logarithm in color flow. It is then possible that it will be cancelled by the corresponding logarithm in the effective diagrams, whose color factor is also C_F . This combination of quark diagrams for achieving factorization also takes place elsewhere. Another triple-gluon vertex correction in Fig. 3(e) involves the invariant masses squared of the virtual quark and of the hard gluon as shown in Eq. (14). At small x , the quark q in Fig. 3(e) is energetic, leading to the collinear logarithmic enhancement $\ln(x_1/\delta_2)$, and the hard gluon has a small invariant mass, leading to the soft enhancement $\ln(x_1/\delta_{12})$. Their overlap then gives rise to the important double logarithm $\ln(x_1/\delta_2) \ln(x_1/\delta_{12})$ in $G_{3e}^{(1)}$. This double logarithm can be reexpressed as

$$2 \ln \frac{x_1}{\delta_2} \ln \frac{x_1}{\delta_{12}} = \ln^2 \frac{x_1}{\delta_2} + \ln^2 \frac{\delta_{12}}{x_1} - \ln^2 \frac{\delta_{12}}{\delta_2}, \quad (16)$$

where the first term, known as the Sudakov logarithm [4, 33], is absorbed into the final-state pion wave function. The Sudakov effect from resumming this double logarithm suppresses the contribution from the small k_{2T} region, i.e., the region with a large impact parameter [5]. The second term $\ln^2(\delta_{12}/x_1) \approx \ln^2 x_2$ also exists in the collinear factorization theorem with k_T being integrated out [34–36]. This threshold logarithm is significant at small x_2 , where the hard gluon approaches mass shell [37]. The third term in Eq. (16) is less important in the small- x region.

There are four box diagrams and two pentagon diagrams as displayed in Fig. 4. Note that Figs. 4(c), 4(e) and 4(f) also contain the corrections to the LO quark diagram Fig. 1(b). As explained in [11], the two-particle reducible diagrams, Figs. 4(a) and 4(e), give power-suppressed contributions at small x . The reason is simply that a collinear or ultraviolet loop momentum increases the virtuality of the LO hard gluons. A soft loop momentum does not change the power-law behavior of the hard kernel, which is, however, not a leading region due to the soft cancellation mentioned before. The expressions for the diagrams other than Figs. 4(a) and 4(e) are collected below:

$$G_{4b}^{(1)} = \frac{\alpha_s}{4\pi N_c} \left[\ln \delta_1 (1 + \ln \delta_2) + 2 \ln x_1 + \frac{\pi^2}{3} - 1 \right] H^{(0)}, \quad (17)$$

$$G_{4c}^{(1)} = -\frac{\alpha_s N_c}{4\pi} \left[\ln \delta_1 (\ln x_1 + 1) - \ln x_2 \left(\frac{3}{2} \ln x_1 + \frac{7}{4} \right) \right] H^{(0)} - \frac{\alpha_s N_c}{4\pi} \left[x_1 \leftrightarrow x_2, \delta_1 \leftrightarrow \delta_2 \right] \bar{H}^{(0)}, \quad (18)$$

$$G_{4d}^{(1)} = -\frac{\alpha_s}{4\pi N_c} \left(\ln \frac{\delta_{12}}{\delta_1} \ln \frac{x_1}{\delta_2} + \frac{\pi^2}{6} \right) H^{(0)}, \quad (19)$$

$$G_{4f}^{(1)} = -\frac{\alpha_s}{4\pi N_c} \left(\ln \frac{\delta_{12}}{x_1 \delta_1} \ln \frac{\delta_{12}}{\delta_2} - \ln 4 - \frac{\pi^2}{4} - \frac{1}{2} \right) H^{(0)} - \frac{\alpha_s}{4\pi N_c} \left(x_1 \leftrightarrow x_2, \delta_1 \leftrightarrow \delta_2 \right) \bar{H}^{(0)}, \quad (20)$$

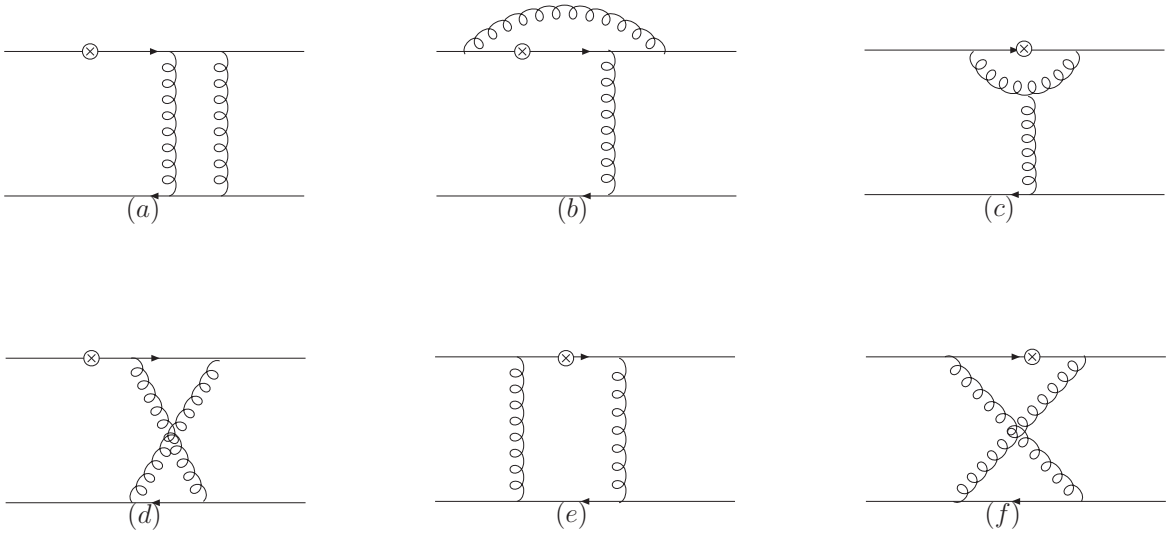


FIG. 4: Box and pentagon diagrams.

with $\bar{H}^{(0)}$ being the LO hard kernel from Fig. 1(b)

$$\bar{H}^{(0)}(x_1, x_2, k_{1T}, k_{2T}, Q^2) = g^2 C_F \frac{\text{Tr}(\not{P}_1 \not{P}_2 \gamma_\mu \not{P}_2)}{Q^2(x_1 x_2 Q^2 + |\mathbf{k}_{1T} - \mathbf{k}_{2T}|^2)}. \quad (21)$$

The above expressions are free of ultraviolet divergences. The correction $G_{4c}^{(1)}$ involves only $\ln \delta_1$, if focusing on the correction to Fig. 1(a), and the important double logarithm $\ln \delta_1 \ln x_1$: $\ln \delta_1$ denotes the collinear enhancement, and $\ln x_1$ denotes the soft enhancement in the small x_1 region. Similarly, the above double logarithm can be reexpressed as

$$2 \ln \delta_1 \ln x_1 = \ln^2 \delta_1 + \ln^2 x_1 - \ln^2 \frac{x_1}{\delta_1}, \quad (22)$$

for the separation the Sudakov logarithm and the threshold logarithm. Figures. 4(b), 4(d), and 4(f), with the soft radiative gluons attaching to the incoming and outgoing partons, generate the soft logarithm $\ln \delta_1 \ln \delta_2$. These soft logarithms cancel among Figs. 3(c), 4(b), 4(d), and 4(f), for the reason that soft gluons do not interact with color-singlet objects like pions.

The sum over all the NLO quark diagrams associated with Fig. 1(a) gives

$$G^{(1)} = \frac{\alpha_s C_F}{4\pi} \left[\frac{21}{4} \left(\frac{1}{\epsilon} + \ln \frac{4\pi\mu^2}{Q^2 e^{\gamma_E}} \right) - 3 \ln(\delta_1 \delta_2) - \frac{9}{4} \ln^2 x_1 + \frac{27}{8} \ln x_1 \ln x_2 + \frac{9}{4} \ln x_1 \ln \delta_{12} \right. \\ \left. + \ln x_1 \left(2 \ln \delta_2 - 2 \ln \delta_1 + \frac{3}{8} \right) + \frac{63}{16} \ln x_2 - \ln \delta_{12} \left(2 \ln \delta_2 + \frac{9}{8} \right) + \frac{1}{2} \ln 2 - \frac{7}{12} \pi^2 + \frac{69}{4} \right] H^{(0)}, \quad (23)$$

for $N_f = 6$. The NLO correction to Fig. 1(b) can be obtained from the above expression by performing the exchanges $x_1 \leftrightarrow x_2$ and $\delta_1 \leftrightarrow \delta_2$.

B. NLO Effective Diagrams

We compute the convolutions of the NLO wave functions $\Phi^{(1)}$ with the LO hard kernel $H^{(0)}$ over the integration variables x' and k'_T ,

$$\Phi_i^{(1)} \otimes H^{(0)} \equiv \int dx'_1 d^2 k'_{1T} \Phi_i^{(1)}(x_1, k_{1T}; x'_1, k'_{1T}) H^{(0)}(x'_1, k'_{1T}, x_2, k_{2T}, Q^2), \\ H^{(0)} \otimes \Phi_i^{(1)} \equiv \int dx'_2 d^2 k'_{2T} H^{(0)}(x_1, k_{1T}, x'_2, k'_{2T}, Q^2) \Phi_i^{(1)}(x_2, k_{2T}; x'_2, k'_{2T}), \quad (24)$$

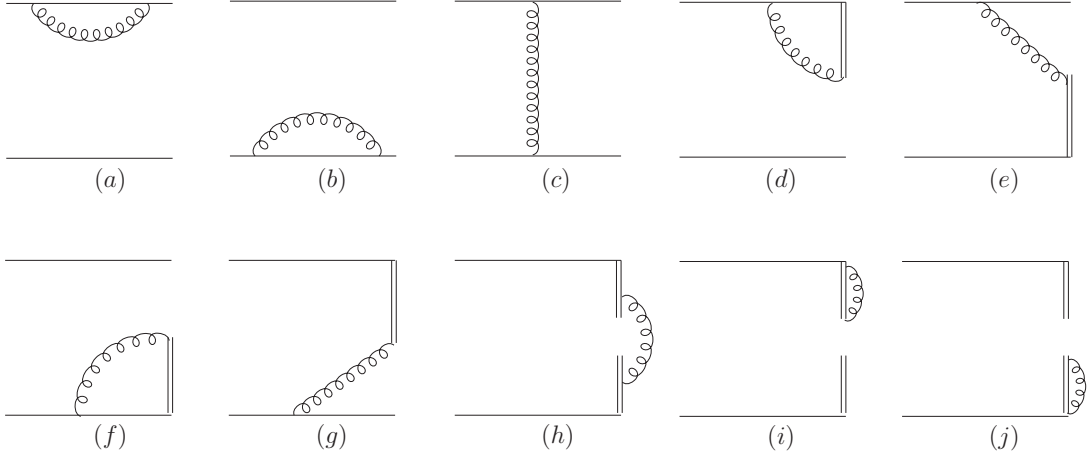


FIG. 5: Effective diagrams.

with a choice of $n^2 \neq 0$ for the Wilson line direction to regularize the light-cone singularities. The NLO wave functions then depend on n^2 through the scale $\zeta_1^2 \equiv 4(n \cdot P_1)^2/|n^2|$ or $\zeta_2^2 \equiv 4(n \cdot P_2)^2/|n^2|$, which is regarded as a factorization-scheme dependence. This dependence, entering a hard kernel when taking the difference between the quark diagrams and the effective diagrams, can be minimized by adhering to a fixed n^2 . Note that the soft subtraction factor introduced in [10] is not necessary here, which is needed for a choice of $n^2 = 0$.

The self-energy corrections from Figs. 5(a) and 5(b) are written as

$$\Phi_a^{(1)} \otimes H^{(0)} = \Phi_b^{(1)} \otimes H^{(0)} = -\frac{\alpha_s C_F}{8\pi} \left(\frac{1}{\epsilon} + \ln \frac{4\pi\mu_f^2}{\delta_1 Q^2 e^{\gamma_E}} + 2 \right) H^{(0)}, \quad (25)$$

$$H^{(0)} \otimes \Phi_a^{(1)} = H^{(0)} \otimes \Phi_b^{(1)} = -\frac{\alpha_s C_F}{8\pi} \left(\frac{1}{\epsilon} + \ln \frac{4\pi\mu_f^2}{\delta_2 Q^2 e^{\gamma_E}} + 2 \right) H^{(0)}, \quad (26)$$

whose expressions are similar to those from the quark diagrams but with the factorization scale μ_f . The contribution from the box diagram in Fig. 5(c) is power-suppressed in the small x region:

$$\Phi_c^{(1)} \otimes H^{(0)} = H^{(0)} \otimes \Phi_c^{(1)} = 0. \quad (27)$$

The sign of the plus component n^+ of the vector n is arbitrary, which could be positive or negative (n^- has a positive sign, the same as of P_2^-). Choosing $n^+ < 0$, i.e., $n^2 < 0$ as in [5, 38, 39], Fig. 5(d) leads, in the small x region, to

$$\begin{aligned} \Phi_d^{(1)} \otimes H^{(0)} &= \frac{\alpha_s C_F}{4\pi} \left(\frac{1}{\epsilon} + \ln \frac{4\pi\mu_f^2}{k_{1T}^2 e^{\gamma_E}} - \ln^2 \frac{\zeta_1^2}{k_{1T}^2} + \ln \frac{\zeta_1^2}{k_{1T}^2} + 2 - \frac{\pi^2}{3} \right) H^{(0)}, \\ H^{(0)} \otimes \Phi_d^{(1)} &= \frac{\alpha_s C_F}{4\pi} \left(\frac{1}{\epsilon} + \ln \frac{4\pi\mu_f^2}{k_{2T}^2 e^{\gamma_E}} - \ln^2 \frac{\zeta_2^2}{k_{2T}^2} + \ln \frac{\zeta_2^2}{k_{2T}^2} + 2 - \frac{\pi^2}{3} \right) H^{(0)}, \end{aligned} \quad (28)$$

which reproduces the Sudakov logarithm in the form of $\ln^2(\zeta^2/k_T^2)$. As computing the convolution of $\Phi_e^{(1)}$ with $H^{(0)}$, the momentum fraction appearing in the hard kernel should be restricted between 0 and 1. The expression for Fig. 5(e) is given, in the small x region, by

$$\begin{aligned} \Phi_e^{(1)} \otimes H^{(0)} &= \frac{\alpha_s C_F}{4\pi} \left[\ln^2 \left(\frac{x_1 \zeta_1^2}{k_{1T}^2} \right) + \frac{2\pi^2}{3} \right] H^{(0)}, \\ H^{(0)} \otimes \Phi_e^{(1)} &= \frac{\alpha_s C_F}{4\pi} \left[\ln^2 \left(\frac{\delta_{12} \zeta_2^2}{x_1 k_{2T}^2} \right) + \frac{2\pi^2}{3} \right] H^{(0)}, \end{aligned} \quad (29)$$

where terms vanishing with $k_T^2 \rightarrow 0$ have been dropped. It is observed that Fig. 5(e) also generates a double logarithm, whose importance is attenuated by the small x .

The result from Fig. 5(f) is similar to that from Fig. 5(d), but with the replacement of $P - k$ by k , i.e., ζ by $x\zeta$. Keeping terms which do not vanish with $k_T^2 \rightarrow 0$, we have

$$\begin{aligned}\Phi_f^{(1)} \otimes H^{(0)} &= \frac{\alpha_s C_F}{4\pi} \left(\frac{1}{\epsilon} + \ln \frac{4\pi\mu_f^2}{k_{1T}^2 e^{\gamma_E}} - \ln^2 \frac{x_1^2 \zeta_1^2}{k_{1T}^2} + \ln \frac{x_1^2 \zeta_1^2}{k_{1T}^2} + 2 - \frac{\pi^2}{3} \right) H^{(0)}, \\ H^{(0)} \otimes \Phi_f^{(1)} &= \frac{\alpha_s C_F}{4\pi} \left(\frac{1}{\epsilon} + \ln \frac{4\pi\mu_f^2}{k_{2T}^2 e^{\gamma_E}} - \ln^2 \frac{x_2^2 \zeta_2^2}{k_{2T}^2} + \ln \frac{x_2^2 \zeta_2^2}{k_{2T}^2} + 2 - \frac{\pi^2}{3} \right) H^{(0)},\end{aligned}\quad (30)$$

where the double logarithm is further attenuated by x^2 . It should disappear, after combined with the contribution from Fig. 5(g), since such a double logarithm is absent in the NLO quark diagrams. The same variable transformation relating $\Phi_f^{(1)}$ to $\Phi_d^{(1)}$ is not applicable to $\Phi_g^{(1)}$, for the latter involves the nontrivial convolution with $H^{(0)}$. Retaining terms which are finite as $k_T \rightarrow 0$, Fig. 5(g) leads to

$$\begin{aligned}\Phi_g^{(1)} \otimes H^{(0)} &= \frac{\alpha_s C_F}{4\pi} \left(\ln^2 \frac{x_1^2 \zeta_1^2}{k_{1T}^2} - \frac{\pi^2}{3} \right) H^{(0)}, \\ H^{(0)} \otimes \Phi_g^{(1)} &= \frac{\alpha_s C_F}{4\pi} \left(\ln^2 \frac{x_2^2 \zeta_2^2}{k_{2T}^2} - \frac{\pi^2}{3} \right) H^{(0)}.\end{aligned}\quad (31)$$

It is easy to see the cancellation of the double logarithms between Eqs. (30) and (31).

At last, we include the self-energy corrections to the Wilson lines, namely, Fig. 5(h-j):

$$\begin{aligned}\Phi_h^{(1)} \otimes H^{(0)} &= \frac{\alpha_s C_F}{2\pi} \left(\frac{1}{\epsilon} + \ln \frac{4\pi\mu_f^2}{\delta_{12} Q^2 e^{\gamma_E}} \right) H^{(0)}, \\ H^{(0)} \otimes \Phi_h^{(1)} &= \frac{\alpha_s C_F}{2\pi} \left(\frac{1}{\epsilon} + \ln \frac{4\pi\mu_f^2}{\delta_{12} Q^2 e^{\gamma_E}} \right) H^{(0)}.\end{aligned}\quad (32)$$

Summing all the above $O(\alpha_s)$ contributions, we obtain

$$\begin{aligned}\Phi^{(1)} \otimes H^{(0)} &= \sum_{i=a}^h \Phi_i^{(1)} \otimes H^{(0)} \\ &= \frac{\alpha_s C_F}{4\pi} \left[\frac{3}{\epsilon} + 3 \ln \frac{4\pi\mu_f^2}{\zeta_1^2 e^{\gamma_E}} + (2 \ln x_1 + 3) \ln \frac{\zeta_1^2}{\delta_1 Q^2} + 2 \ln \frac{\zeta_1^2}{\delta_{12} Q^2} + \ln x_1 (\ln x_1 + 2) + 2 - \frac{\pi^2}{3} \right] H^{(0)}, \\ H^{(0)} \otimes \Phi^{(1)} &= \sum_{i=a}^h H^{(0)} \otimes \Phi_i^{(1)} \\ &= \frac{\alpha_s C_F}{4\pi} \left[\frac{3}{\epsilon} + 3 \ln \frac{4\pi\mu_f^2}{\zeta_2^2 e^{\gamma_E}} + (2 \ln \frac{\delta_{12}}{x_1} + 3) \ln \frac{\zeta_2^2}{\delta_2 Q^2} + 2 \ln \frac{\zeta_2^2}{\delta_{12} Q^2} + \ln^2 \frac{\delta_{12}}{x_1} + 2 \ln x_2 + 2 - \frac{\pi^2}{3} \right] H^{(0)}.\end{aligned}\quad (33)$$

The resultant anomalous dimension of the pion wave function is the same as derived in the axial gauge (for a recent reference, see [31]).

C. NLO Hard Kernel

We derive the NLO hard kernel for the pion electromagnetic form factor in the k_T factorization theorem by taking the difference between the quark and effective diagrams. Note that α_s appearing in Eqs. (23) and (33) denotes the bare coupling constant, which can be rewritten as

$$\alpha_s = \alpha_s(\mu_f) + \delta Z(\mu_f) \alpha_s(\mu_f), \quad (34)$$

with the counterterm δZ being defined in the modified minimal subtraction scheme. We insert Eq. (34) into the expressions of the LO and NLO quark diagrams, and of the NLO effective diagrams. The LO hard kernel $H^{(0)}$ multiplied by δZ then regularizes the ultraviolet pole in Eq. (23). The ultraviolet pole in Eq. (33) is regularized by the counterterm of the quark field and by an additive counterterm in the modified minimal subtraction scheme. For the infrared logarithms, there exists a cancellation between the two-particle reducible quark diagrams and the two-particle

reducible effective diagrams. That is, $G_{2a,2b}^{(1)} - H^{(0)} \otimes \Phi_{a,b}^{(1)}$ and $G_{2c,2d}^{(1)} - \Phi_{a,b}^{(1)} \otimes H^{(0)}$ are infrared finite. The self-energy diagrams for the internal quarks and gluons are free of infrared divergences. The collinear logarithm represented by $\ln \delta_1$ ($\ln \delta_2$) cancels between the two-particle irreducible diagrams and the convolution $[\Phi_d^{(1)} + \Phi_e^{(1)} + \Phi_f^{(1)} + \Phi_g^{(1)}] \otimes H^{(0)}$ ($H^{(0)} \otimes [\Phi_d^{(1)} + \Phi_e^{(1)} + \Phi_f^{(1)} + \Phi_g^{(1)}]$).

The infrared-finite k_T -dependent NLO hard kernel for Fig. 1(a) is given by

$$H^{(1)} = \frac{\alpha_s(\mu_f)C_F}{4\pi} \left(\frac{21}{4} \ln \frac{\mu^2}{Q^2} - 6 \ln \frac{\mu_f^2}{Q^2} - \frac{17}{4} \ln^2 x_1 + \frac{27}{8} \ln x_1 \ln x_2 - \ln^2 \delta_{12} + \frac{17}{4} \ln x_1 \ln \delta_{12} - \frac{13}{8} \ln x_1 + \frac{31}{16} \ln x_2 + \frac{23}{8} \ln \delta_{12} + \frac{1}{2} \ln 2 + \frac{5\pi^2}{48} + \frac{53}{4} \right) H^{(0)}. \quad (35)$$

We have chosen $|n^+| = n^-$, which renders $\zeta^2 = Q^2$, to avoid creating an additional large logarithm like $\ln(\zeta^2/Q^2)$. The Sudakov logarithm $\ln^2(Q^2/k_T^2)$ in Eq. (22) has been removed by that in the effective diagrams, but the threshold logarithms $\ln^2 x^2$ remains in $H^{(1)}$, which can be absorbed into a jet function [37]. Because there is no end-point singularity in the pion form factor at twist-2, we shall not perform the factorization of this threshold logarithm here. However, an end-point singularity does exist in the contribution from the two-parton twist-3 pion distribution amplitudes, so the factorization and the threshold resummation for the jet function needs to be performed.

We have checked that Eq. (35) is gauge-invariant by repeating the NLO calculations in an arbitrary covariant gauge. Applying the Ward identity to the gauge-dependent terms [11, 12], it is easy to show that the gauge dependence cancels between the quark diagrams and the effective diagrams. The NLO hard kernel $\bar{H}^{(1)}$ for Fig. 1(b) can be obtained from Eq. (35) by exchanging x_1 and x_2 , and by substituting $\bar{H}^{(0)}$ in Eq. (21) for $H^{(0)}$. The NLO hard kernels for the other two LO quark diagrams with the virtual photon attaching to the anti-quark line can be obtained from $H^{(1)}$ and $\bar{H}^{(1)}$ by exchanging x and $1-x$.

III. NUMERICAL ANALYSIS

In this section we evaluate the NLO correction to the pion electromagnetic form factor in the k_T factorization theorem numerically. Since the Sudakov suppression was derived in the impact parameter space, we write the factorization formula as a convolution in the impact parameters b_1 and b_2 [5], conjugate to k_{1T} and k_{2T} , respectively. The Sudakov factor, resulting from the summation of the double logarithm $\alpha_s \ln^2 k_T$ to all orders, describes the perturbative k_T dependence of a pion wave function. We shall not consider the intrinsic k_T dependence of a pion wave function proposed in [40] here. To simplify the expression of the NLO hard kernel in the b_1 - b_2 space, we adopt the approximation $\ln \delta_{12} \approx \ln(x_1 x_2)$. This approximation does not modify the power-law behavior of end-point contributions from small x , and affects numerical outcomes only slightly. We first test the following asymptotic models for the twist-2 pion distribution amplitude ϕ_π^A and the two-parton twist-3 pion distribution amplitudes $\phi_\pi^{P,T}$,

$$\begin{aligned} \phi_\pi^A(x) &= \frac{6f_\pi}{2\sqrt{2}N_c} x(1-x), \\ \phi_\pi^P(x) &= \frac{f_\pi}{2\sqrt{2}N_c}, \\ \phi_\pi^T(x) &= \frac{f_\pi}{2\sqrt{2}N_c} (1-2x), \end{aligned} \quad (36)$$

where the pion decay constant is taken as $f_\pi = 130$ MeV.

The first issue concerns the choice of the renormalization scale μ and the factorization scale μ_f in order to minimize the NLO correction to the pion form factor. The results are summarized in Fig. 6, which displays the ratio of the NLO contribution over the LO one as a function of Q^2 . For the first choice, μ_f is set to the hard scale t defined in the PQCD approach to exclusive processes based on the k_T factorization theorem [5, 25]

$$t = \max(\sqrt{x}Q, 1/b_1, 1/b_2). \quad (37)$$

Then we utilize the freedom of choosing μ to diminish all the single-logarithmic and constant terms in the NLO hard kernel, which is found to be

$$t_s(\mu_f) = \exp\left(\frac{53}{42} + \frac{5\pi^2}{504}\right) x_1^{5/42} x_2^{11/24} \left(\frac{\mu_f}{Q}\right)^{1/7} \mu_f. \quad (38)$$

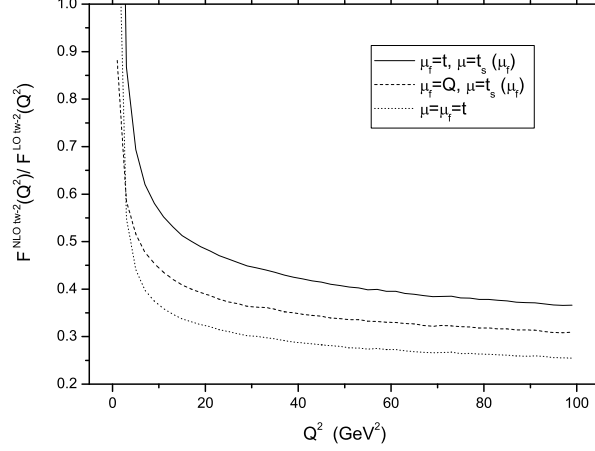


FIG. 6: Ratio of the NLO correction over the LO contribution to the pion form factor with the scale $t_s(\mu_f)$ being defined in Eq. (38).

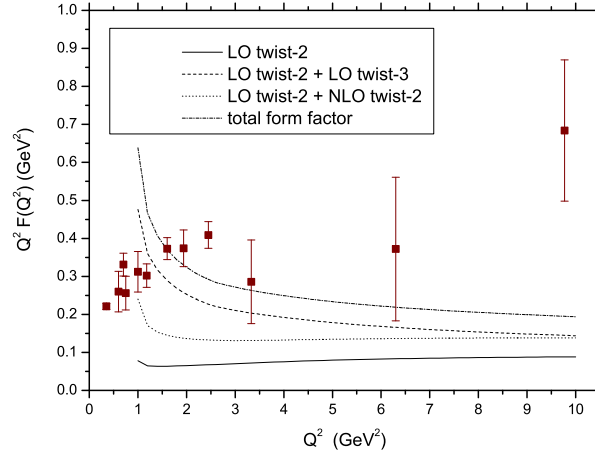


FIG. 7: Pion form factor from different orders and twists for the asymptotic pion distribution amplitudes in Eq. (36). The experimental data are taken from [41] and [42].

This scale choice gives a larger NLO correction: the NLO correction becomes less than 40% of the LO contribution only when Q^2 is higher than 55 GeV². The second choice corresponds to $\mu_f = Q$, which is greater than t , and $\mu = t_s$, which removes all the single-logarithmic and constant terms in the NLO hard kernel. The convergence of the NLO correction is improved: the NLO correction becomes less than 40% as $Q^2 > 17$ GeV². The third choice is the conventional one adopted in the PQCD approach to exclusive processes, with both μ and μ_f being set to t . It turns out that this simple choice works better: the NLO correction becomes less than 40% as $Q^2 > 7$ GeV². The above analysis confirms the prescription postulated in [5] that both the renormalization and factorization scales are set to the invariant masses of internal particles.

After fixing the scales, we calculate the LO twist-2, NLO twist-2, and LO two-parton twist-3 contributions to the pion form factor, and present the results in Fig. 7. Note that the last piece of contribution involves two two-parton twist-3 pion distribution amplitudes, so it is suppressed by a power of $1/Q^2$. Figure 7 indicates that the LO twist-2 contribution is quite small compared to the experimental data in the whole considered range of Q^2 . The NLO twist-2 contribution is also small, and helps to explain the data only at $Q^2 \sim 1$ GeV², where the perturbation theory may

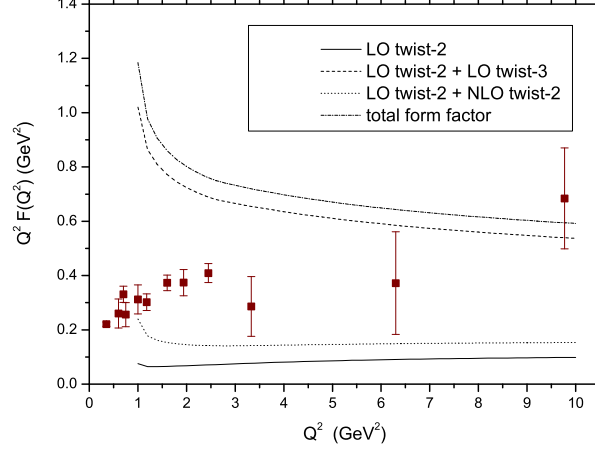


FIG. 8: Contributions to the pion form factor from different orders and twists for the non-asymptotic models in Eq. (39).

not be reliable: the quick growth of our results at very low Q^2 is attributed to the presence of the infrared Landau pole in the strong coupling constant. To study the pion form factor in this region, a soft contribution is needed, and an analytic perturbation theory may help [43]. The LO two-parton twist-3 contribution dominates in most range of Q^2 , and becomes comparable to the NLO twist-2 one as $Q^2 \sim 10 \text{ GeV}^2$. The dominance comes from the chiral enhancement scale $m_0(1\text{GeV}) = 1.74 \text{ GeV}$, which is of the same order of magnitude as low Q values. With this contribution being included, it is possible to accommodate the data in the large Q^2 region. It supports the treatment in the PQCD approach to exclusive B meson decays [25], in which the NLO twist-2 correction to B transition form factors is neglected, but the LO two-parton twist-3 one is included. That is, the latter should be the most important subleading contribution. The recent BaBar data for the pion transition form factor at low Q^2 favors an asymptotic pion distribution amplitude [27]. Figure 7 implies that the data of the pion form factor at low Q^2 also support the asymptotic models for the pion distribution amplitudes. Besides, the asymptotic models are favored from the viewpoint of light-cone sum rules, which reproduce the data of the pion form factor [23]. As pointed out in [44], the experimental data of $F(Q^2)$ at higher Q^2 from [42] have large additional uncertainties due to the model dependent subtraction of transverse cross section, on top of the large statistical and systematic errors. Therefore, no conclusive statement on the agreement or disagreement between data and theory can be made.

It is interesting to examine whether the shape of the pion distribution amplitudes matters for explaining the data, an issue that has been investigated and discussed in various aspects intensively. We test the following non-asymptotic pion distribution amplitudes [45]:

$$\begin{aligned}
 \phi_\pi^A(x) &= \frac{6f_\pi}{2\sqrt{2N_c}}x(1-x)[1 + 0.16C_2^{3/2}(u) + 0.04C_4^{3/2}(u)], \\
 \phi_\pi^P(x) &= \frac{f_\pi}{2\sqrt{2N_c}}[1 + 0.59C_2^{1/2}(u) + 0.09C_4^{1/2}(u)], \\
 \phi_\pi^T(x) &= \frac{f_\pi}{2\sqrt{2N_c}}[C_1^{1/2}(u) + 0.019C_3^{1/2}(u)],
 \end{aligned} \tag{39}$$

with the Gegenbauer polynomials

$$\begin{aligned}
 C_1^{1/2}(u) &= u, & C_3^{1/2}(u) &= \frac{1}{2}u(5u^2 - 3), \\
 C_2^{1/2}(u) &= \frac{1}{2}(3u^2 - 1), & C_4^{1/2}(u) &= \frac{1}{8}(35u^4 - 30u^2 + 3), \\
 C_2^{3/2}(u) &= \frac{3}{2}(5u^2 - 1), & C_4^{3/2}(u) &= \frac{15}{8}(21u^4 - 14u^2 + 1),
 \end{aligned} \tag{40}$$

and the variable $u = 1 - 2x$. Figure 8 shows that the above models overshoot the data in the small Q^2 region. Hence, the matrix elements of higher conformal spin operators may have been overestimated in [45].

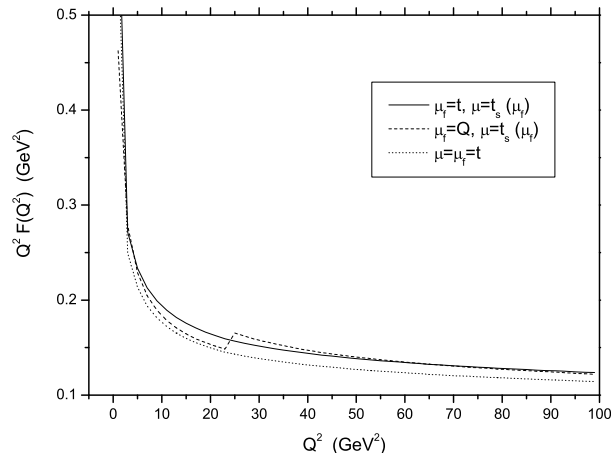


FIG. 9: Scale dependence of the pion form factor with $t_s(\mu_f)$ being defined in Eq. (38).

At last, we investigate the theoretical uncertainty in our calculation by studying the scale dependence, and the results are presented in Fig. 9. The curves corresponding to $\mu_f = t$, $\mu = t_s$ and $\mu_f = \mu = t$ differ by about 10% in the considered range of Q^2 , implying that the theoretical uncertainty is under control. The sharp jump exhibited by the curve corresponding to $\mu_f = Q$, $\mu = t_s$ is attributed to the change of the QCD scale Λ_{QCD} with the upper bounds of the integration variables b_1 and b_2 . When the momentum transfer squared increases up to $Q^2 = 23 \text{ GeV}^2$, the value $\Lambda_{\text{QCD}}^{(4)} = 286 \text{ MeV}$ is replaced by $\Lambda_{\text{QCD}}^{(5)} = 204 \text{ MeV}$, and the sharp jump is produced as shown in Fig. 9. This jump is not obvious for $\mu_f = t$ (the other two curves), whose value is typically smaller than Q , so it does not excite $\Lambda_{\text{QCD}}^{(4)}$ to $\Lambda_{\text{QCD}}^{(5)}$ at $Q^2 = 23 \text{ GeV}^2$.

IV. CONCLUSION

In this paper we have extended the framework for higher-order calculations in the k_T factorization theorem to the pion electromagnetic form factor. The prescription is that partons in both QCD quark diagrams and effective diagrams for TMD hadron wave functions are off mass shell by k_T^2 . The light-cone divergences in naive definitions of TMD hadron wave functions were regularized by rotating the Wilson lines away from the light cone. Since the k_T factorization theorem is appropriate for QCD processes dominated by contributions from small momentum fractions, terms suppressed by powers of momentum fractions have been neglected, and simple expressions can be obtained for the box and pentagon diagrams. We have demonstrated the disappearance of the soft logarithms, and the exact cancellation of the collinear logarithms in the difference of the quark and effective diagrams. Our work represents the first NLO analysis of the pion form factor in the k_T factorization theorem.

Our numerical study has indicated that setting the renormalization and factorization scales to invariant masses of internal particles reduces NLO corrections. The NLO correction to the pion form factor becomes lower than 40% of the LO one for $Q^2 > 7 \text{ GeV}^2$. This observation supports the conventional scale choice adopted in the PQCD approach to exclusive processes based on the k_T factorization theorem, and is consistent with that made in the collinear factorization theorem [22]. We have found that the NLO twist-2 contribution does not help accommodating the data of the pion form factor. Instead, the LO two-parton twist-3 contribution plays a crucial role for the purpose. It is also confirmed that the asymptotic pion distribution amplitudes are favored by the data available at low Q^2 . Comparing the results from the different choices of the renormalization and factorization scales, the theoretical uncertainty in our calculation is estimated to be around 10%. We shall apply the same framework to the NLO analysis of B meson transition form factors in a forthcoming paper.

The work was supported in part by the National Science Council of R.O.C. under Grant No. NSC-98-2112-M-001-015-MY3, by the National Center for Theoretical Sciences of R.O.C., by National Science Foundation of China under Grant No. 11005100, and by the the Deutsche Forschungsgemeinschaft under Contract No. KH205/1-2. Y.M.W.

would like to acknowledge Prof. Cai-Dian Lü for warm hospitality during his visit at IHEP, Beijing, and Prof. Xue-Qian Li for inviting him to give a talk at Nankai University.

-
- [1] S. Catani, M. Ciafaloni and F. Hautmann, Phys. Lett. B **242**, 97 (1990); Nucl. Phys. B **366**, 135 (1991).
 - [2] J.C. Collins and R.K. Ellis, Nucl. Phys. B **360**, 3 (1991).
 - [3] E.M. Levin, M.G. Ryskin, Yu.M. Shabelskii, and A.G. Shuvaev, Sov. J. Nucl. Phys. **53**, 657 (1991).
 - [4] J. Botts and G. Sterman, Nucl. Phys. B **225**, 62 (1989).
 - [5] H-n. Li and G. Sterman, Nucl. Phys. B **381**, 129 (1992).
 - [6] T. Huang and Q.X. Shen, Z. Phys. C **50**, 139 (1991); J.P. Ralston and B. Pire, Phys. Rev. Lett. **65**, 2343 (1990).
 - [7] F. Dominguez, B.W. Xiao, and F. Yuan, Phys. Rev. Lett. **106**, 022301 (2011).
 - [8] S.P. Baranov, A.V. Lipatov, and N.P. Zotov, arXiv:1012.3022 [hep-ph]; A.V. Lipatov, M.A. Malyshev, and N.P. Zotov, arXiv:1102.1134 [hep-ph].
 - [9] M. Nagashima and H-n. Li, Phys. Rev. D **67**, 034001 (2003).
 - [10] F. Feng, J. P. Ma and Q. Wang, Phys. Lett. B **674**, 176 (2009).
 - [11] S. Nandi and H-n. Li, Phys. Rev. D **76**, 034008 (2007).
 - [12] H-n. Li and S. Mishima, Phys. Lett. B **674**, 182 (2009).
 - [13] J.C. Collins, Acta. Phys. Polon. B **34**, 3103 (2003).
 - [14] J.P. Ma and Q. Wang, JHEP **0601**, 067 (2006); Phys. Lett. B **642**, 232 (2006).
 - [15] H-n. Li and H.S. Liao, Phys. Rev. D **70**, 074030 (2004).
 - [16] R.D. Field, R. Gupta, S. Otto, and L. Chang, Nucl. Phys. B **186**, 429 (1981).
 - [17] F.M. Dittes and A.V. Radyushkin, Yad. Fiz. **34**, 529 (1981) [Sov. J. Nucl. Phys. **34**, 293 (1981)].
 - [18] M.H. Sarmadi, Ph.D. thesis, University of Pittsburgh, 1982.
 - [19] R.S. Khalmuradov and A.V. Radyushkin, Yad. Fiz. **42**, 458 (1985), [Sov. J. Nucl. Phys. **42**, 289 (1985)].
 - [20] E. Braaten and S.M. Tse, Phys. Rev. D **35**, 2255 (1987).
 - [21] E.P. Kadantseva, S.V. Mikhailov, and A.V. Radyushkin, Yad. Fiz. **44**, 507 (1986) [Sov. J. Nucl. Phys. **44**, 326 (1986)].
 - [22] B. Melic, B. Nizic, and K. Passek, Phys. Rev. D **60**, 074004 (1999).
 - [23] V. M. Braun, A. Khodjamirian and M. Maul, Phys. Rev. D **61**, 073004 (2000).
 - [24] J. Bijnens and A. Khodjamirian, Eur. Phys. J. C **26**, 67 (2002).
 - [25] Y.Y. Keum, H-n. Li, and A.I. Sanda, Phys. Lett. B **504**, 6 (2001); Phys. Rev. D **63**, 054008 (2001); Y.Y. Keum and H-n. Li, Phys. Rev. D **63**, 074006 (2001); C. D. Lu, K. Ukai and M. Z. Yang, Phys. Rev. D **63**, 074009 (2001).
 - [26] H-n. Li and S. Mishima, Phys. Rev. D **80**, 074024 (2009).
 - [27] B. Aubert *et al.* [The BABAR Collaboration], Phys. Rev. D **80**, 052002 (2009).
 - [28] Z.T. Wei and M.Z. Yang, Phys. Rev. D **67**, 094013 (2003); J.W. Chen, H. Kohyama, K. Ohnishi, U. Raha, and Y.L. Shen, Phys. Lett. B **693**, 102 (2010).
 - [29] H-n. Li, Phys. Rev. D **64**, 014019 (2001); M. Nagashima and H-n. Li, Eur. Phys. J. C **40**, 395 (2005).
 - [30] X. Ji, and F. Yuan, Phys. Lett. B **543**, 66 (2002); A.V. Belitsky, X. Ji, and F. Yuan, Nucl. Phys. B **656**, 165 (2003).
 - [31] I. O. Cherednikov and N. G. Stefanis, Nucl. Phys. B **802**, 146 (2008).
 - [32] W. Siegel, Phys. Lett. B **84**, 193 (1979).
 - [33] J.C. Collins and D.E. Soper, Nucl. Phys. B **193**, 381 (1981).
 - [34] G.P. Korchemsky, D. Pirjol, and T.M. Yan, Phys. Rev. D **61**, 114510 (2000) and references therein.
 - [35] J.P. Ma and Q. Wang, Phys. Rev. D **75**, 014014 (2007) and references therein.
 - [36] R. Akhoury, G. F. Sterman and Y. P. Yao, Phys. Rev. D **50**, 358 (1994).
 - [37] H-n. Li, Phys. Rev. D **66**, 094010 (2002); K. Ukai and H-n. Li, Phys. Lett. B **555**, 197 (2003).
 - [38] H-n. Li and H.L. Yu, Phys. Rev. Lett. **74**, 4388 (1995); Phys. Lett. B **353**, 301 (1995); Phys. Rev. D **53**, 2480 (1996).
 - [39] H-n. Li, Phys. Rev. D **55**, 105 (1997).
 - [40] R. Jakob and P. Kroll, Phys. Lett. B **315**, 463 (1993); B **319**, 545 (1993)(E).
 - [41] G. M. Huber *et al.* [Jefferson Lab Collaboration], Phys. Rev. C **78**, 045203 (2008).
 - [42] C. J. Bebek *et al.*, Phys. Rev. D **17**, 1693 (1978).
 - [43] A. P. Bakulev, K. Passek-Kumericki, W. Schroers and N. G. Stefanis, Phys. Rev. D **70**, 033014 (2004) [Erratum-ibid. D **70**, 079906 (2004)].
 - [44] H. P. Blok, G. M. Huber and D. J. Mack, arXiv:nucl-ex/0208011.
 - [45] G. Duplancic, A. Khodjamirian, T. Mannel, B. Melic, and N. Offen, JHEP **0804**, 014 (2008).